JOURNAL OF GEOPHYSICAL RESEARCH, VOL. 103, NO. A11, PAGES 26,859–26,868, NOVEMBER 1, 1998

Sector boundary transformation by an open magnetic cloud

N. U. Crooker,[1] A. H. McAllister,[2] R. J. Fitzenreiter,[3] J. A. Linker,[4] D. E. Larson,[5]
R. P. Lepping,[3] A. Szabo,[3] J. T. Steinberg,[6] A. J. Lazarus,[6]
Z. Mikic,[4] and R. P. Lin[5]

Abstract. A magnetic cloud observed by the Wind spacecraft on February 8, 1995, was remarkable for its impact on the interplanetary sector structure. The magnetic field data imply that the cloud occurred in the middle of a sector and that the arrival of the following sector boundary on February 10 coincided with the arrival time predicted from the corresponding source surface map. The electron heat flux data, however, give incontrovertible evidence that instead the cloud brought the sector boundary, well ahead of the predicted arrival time. The electron heat flux data show little counterstreaming within the cloud, indicating predominantly open helical field lines. Under the assumption that the cloud originally had the form of a closed flux rope loop with legs rooted to the Sun, observational constraints dictate that the sector boundary was displaced not because it was pushed aside by the cloud but because reconnection in the leading leg opened field lines there, creating a topological change spanning 45° of heliographic longitude. The solar source of the cloud was deduced from an associated eruptive arcade event extending northeastward from an active region in Yohkoh soft X ray data on February 4. On February 8, the same active region was the source of impulsive energetic electron events observed at Wind during a brief counterstreaming interval, consistent with magnetic connection in the leading leg at that time. The cloud's helicity matches that predicted from the skew of the arcade fields in the February 4 X ray event, but the predicted alignment of the arcade and cloud axes was off by 35°. We use an MHD model with boundary conditions derived from solar magnetograms to illustrate the tilted arcade configuration in the corona that gave rise to the magnetic cloud and the lesser tilt of the heliospheric current sheet stemming from it.

1. Introduction

Although the relationship between magnetic clouds and sector boundaries seems obvious in the context of basic heliospheric topology [e.g., *Crooker et al.*, 1993; *Zhao and Hoeksema*, 1996], briefly described below, from the perspective of interplanetary measurements the relationship has been unclear for at least two reasons. First, the interplanetary signatures of clouds are usually complicated, and, second, only about half of observed magnetic clouds can even be associated with sector boundaries [*Bothmer and Schwenn*, 1998; *Crooker et al.*, 1998]. For the associated cases, however, *Crooker et al.* [1998] have identified a repeatable pattern consistent with basic heliospheric topology. The present study builds on those results by analyzing a magnetic cloud with markedly different characteristics and, with the aid of data from its associated solar source, demonstrating how it, too, fits into the basic topology. In so doing, the study reveals how sector boundaries can be dramatically altered during cloud passage.

Since the interpretation of the present results depends on an understanding of how the clouds observed at sector boundaries appear to fit into the basic topology of the heliosphere, we review here the findings of *Crooker et al.* [1998]. Figure 1, adapted from their paper, schematically illustrates their concluding interpretation. We describe the features in the figure first and then discuss how they fit both the basic heliospheric topology and the ISEE 3 observations. Figure 1 shows an ecliptic view of a flux rope representing a magnetic cloud approaching 1 AU. The rope is connected to the Sun at both ends, with one end connected above the ecliptic plane and the other below it. The rope forms a loop, as indicated by the projection onto the ecliptic plane of the singular nonhelical field line that constitutes the rope axis. The shaded area represents the ecliptic cross section of the rope. It does not extend all the way to the Sun owing to the assumed, gentle tilt of the plane of the axis of the loop with respect to the ecliptic plane. The flux rope loop is drawn to roughly follow the Parker spiral, as indicated by the shape of the axis field line and the cross section. Thus the view is kinematic and does not take into account magnetic forces which would tend to push the legs apart to form a more rounded loop [cf. *Marubashi*, 1997]. (To what extent rounding might occur is not clear, since the solar wind expansion speed is much larger than the Alfven speed by which magnetic forces are communicated.) The black dots indicate

[1]Center for Space Physics, Boston University, Boston, Massachusetts.
[2]Helio Research, La Crescenta, California.
[3]Laboratory for Extraterrestrial Physics, NASA Goddard Space Flight Center, Greenbelt, Maryland.
[4]Science Applications International Corporation, San Diego, California.
[5]Space Sciences Laboratory, University of California, Berkeley.
[6]Center for Space Research, Massachusetts Institute of Technology, Cambridge.

Paper number 98JA02391.
0148-0227/98/98JA-02391$09.00

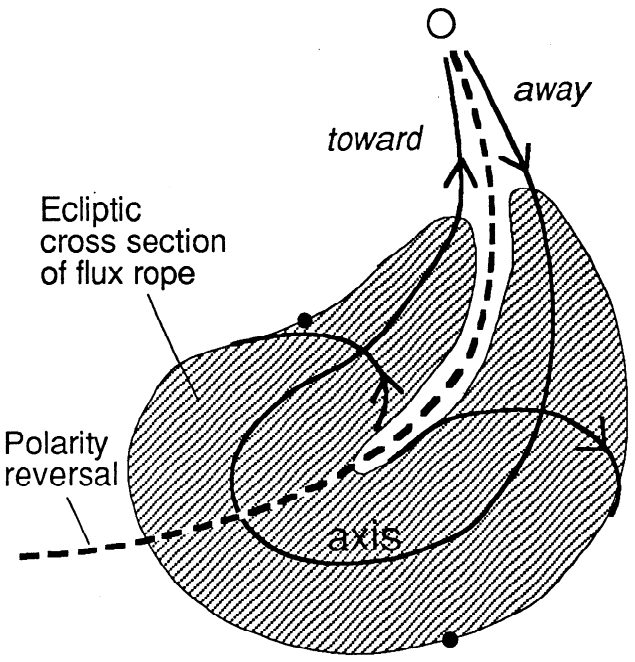

Figure 1. Schematic illustration of a coronal mass ejection (CME) flux rope loop in the context of the associated sector boundary. The rope is attached to the Sun at both ends and distorted along the Parker spiral so that spacecraft passage through both the leading and trailing portions yields a double rope signature on closed field lines. Black dots roughly indicate spacecraft entry and exit points (see text). The hatched ecliptic cross section does not connect to the Sun owing to an assumed tilt of the plane of the loop axis, which is projected onto the figure. Two sample helical field segments near the rope's surface point in the direction of the solar dipolar component on the outside of the loop, consistent with a helmet arcade origin in the streamer belt. The loop forms a distorted bubble in the heliospheric current sheet, but a magnetic polarity reversal would be detected in the ecliptic plane along the dashed curve irrespective of whether the spacecraft was within or outside the loop (adapted from *Crooker et al.* [1998]).

possible entry and exit points of a spacecraft through the flux rope loop. The dots are not radially aligned because the base of the loop corotates with the Sun and the shape of the structure changes during spacecraft passage [see *Crooker et al.*, 1998].

The Figure 1 flux rope fits into basic heliospheric topology as modeled, for example, by *Pneuman and Kopp* [1971]. It is drawn to be consistent with flux rope formation under the helmet streamer arcade that encircles the Sun as a belt at the base of the heliospheric current sheet (HCS) (illustrated in Figure 1 of *Crooker et al.* [1998]). The streamer belt source for the flux rope is based on the extensive observations of coronal mass ejection (CME) formation there [e.g., *Hundhausen*, 1993; *McAllister and Hundhausen*, 1996; *Howard et al.*, 1997]. The arcade field lines in the helmet streamer belt are dominated by the dipolar component of the Sun's magnetic field. After assumed reconnection of the arcade fields beneath the rope at CME liftoff [e.g., *Martin and McAllister*, 1997, 1998], the arcade fields become helical and coat the surface of the rope in Figure 1. Around the outer boundary of the loop, the two samples shown thus point in the direction of the solar dipole field, assumed southward in this case, and inside the loop they point in the opposite direction, northward. Near the Sun the rope axis is perpendicular to the arcade fields and parallel to the neutral line threading the arcade and to the HCS stemming from its apex. As the rope axis becomes a loop in space, the orientation of its leading edge is assumed to be maintained so that the tilt of the plane of the loop matches the tilt of the neutral line and the inclination of the HCS [e.g., *Zhao and Hoeksema*, 1996]. The flux rope axis thus lies in the plane of the global scale HCS, and the rope itself creates a loop-shaped bubble or occlusion in the HCS [*Crooker and Intriligator*, 1996].

The magnetic polarity reversal associated with the sector boundary in the ecliptic plane, indicated by the dashed curve, runs through the center of the flux rope loop, under the assumption that the flux rope is centered on the ecliptic plane. This location may at first appear surprising in view of the helical, non-Parker-spiral fields within the rope. Except for the outermost coils, however, the helical fields all carry at least a small component parallel to the direction of the field along the axis. It then follows from the Parker spiral alignment of the loop legs that the measured magnetic longitude would gradually rotate from away to toward polarity as the structure passed over a spacecraft, as often observed across magnetic clouds at sector boundaries [e.g., *Crooker et al.*, 1998]. Thus the magnetic polarity reversal occurs at the dashed line independent of whether the fields are open or closed, helical or Parker spiraled. The sector structure is maintained whether the current is carried in a sheet or distributed through a flux rope [cf. *Burton et al.*, 1994; *Zhao and Hoeksema*, 1996; *Kahler et al.*, 1996]. The sense of the polarity reversal in Figure 1 combined with the direction of the dipolar arcade fields coating the flux rope surface requires that the plane of the rope axis in this case be tilted slightly downward to the right so that passage is from above to below the HCS.

Two features of most of the magnetic clouds observed at sector boundaries by ISEE 3 fit the Figure 1 pattern [*Crooker et al.*, 1998], First, counterstreaming electrons signaling closed magnetic structure extended well beyond the trailing boundary of the originally identified clouds. Second, the magnetic field during the counterstreaming intervals rotated through what roughly appeared to be double flux rope signatures, characterized by arched variations in the magnetic latitude angle, from negative to positive to negative values, or vice versa. Based on these findings, *Crooker et al.* [1998] suggested that the originally identified clouds with their single flux rope signatures were only the leading portion of flux rope loops and that, following *Marubashi* [1997], spacecraft passage through the trailing legs of the loops, as well, yielded the double rope signatures, as Figure 1 illustrates.

In section 2 we present data from a magnetic cloud and associated sector boundary that seem like a puzzling departure from the Figure 1 structure, but in section 3 we show how an interpretation in terms of a closely related structure fits the data. In section 4 we identify the solar source of the cloud and evaluate the degree to which cloud properties match those of the source.

2. The February 8 Cloud and Surrounding Sector Structure

Lepping et al. [1996a] first identified the February 8, 1995, magnetic cloud in Wind data for a comparative study with IMP 8 data, and *Lepping et al.* [1996b] documented the interplanetary magnetic sector structure for early 1995. Both the cloud and the sector structure are indicated in the 27-day plot of the

magnetic longitude angle ϕ from the Wind Magnetic Field Investigation (MFI) in Figure 2a, where time runs from right to left. The horizontal dotted lines mark the angles 45° and 225° that separate fields pointing toward the Sun along the Parker spiral from those pointing away, and shading indicates toward sectors. (Additional shading used by *Lepping et al.* [1996b] to mark intervals of multiple polarity changes, some of which are present only in the higher-resolution data, has been omitted for clarity.) The hatched column marking the magnetic cloud indicates that it appeared to occur in the middle of an away sector.

The midsector location of the cloud agrees with the sector structure predicted from the Wilcox Observatory source surface map of the coronal magnetic field in Figure 2b. The map is aligned with the plot of ϕ above it, taking into account a solar wind lag time of 4 1/2 days between the Sun and the Wind spacecraft. The heavy dashed line on the map marks the ecliptic path of Wind across it, and its intersection with the heavy neutral line marks the predicted sector boundary location. The predictions provide a good match to the magnetic polarity changes on February 4 and 10 in Figure 2a, as indicated by the outer two lines connecting the panels. Although below we show that the magnetic polarity change on February 10 is not a true polarity change, in section 3 we argue that the match with the prediction from the source surface map is not serendipitous but rather an expected result.

Of the remaining two sector boundary crossings in Figure 2, the February 16 crossing matches the neutral line prediction reasonably well, but the February 26 crossing does not. Interestingly, the partial crossing on February 23 matches better

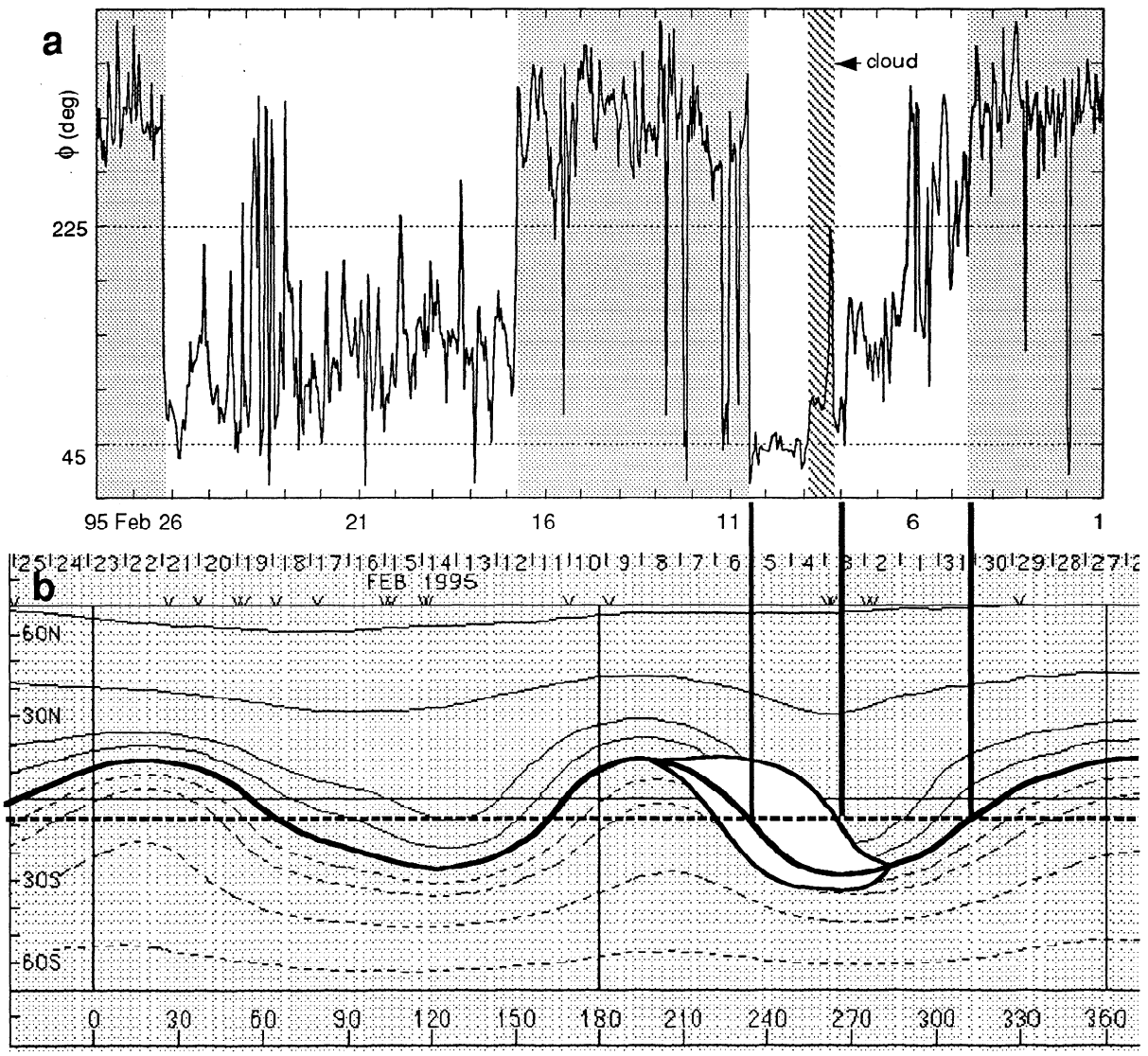

Figure 2. (a) Right-to-left time variation of magnetic longitude angle ϕ (GSE coordinates) and (b) map of the coronal source surface field from the Wilcox Solar Observatory (World Wide Web) for Carrington Rotation 1892, aligned with a 4 1/2 - day lag. The outer two of the three thick vertical lines match the first two sector boundaries determined from ϕ with neutral line predictions from the map, where the dashed line indicates the path of Wind across the map. The cloud, which appears to occur in the middle of a sector, brought the true sector boundary early, at its leading edge, indicated by the middle thick vertical line. Observations in Figure 4 combined with results from *Crooker et al.* [1998] suggest that the cloud was the leading portion of a flux rope loop that formed a bubble in the HCS, indicated by the outlined expansion of the neutral line.

and may be associated with another transient structure. This feature, however, is beyond the scope of the present study.

The true polarity of a field line can be different from its local orientation at a spacecraft if the field line folds back on itself [*Kahler and Lin*, 1994, 1995]. True polarity can be determined by observing the direction of the electron heat flux relative to the field direction [*Kahler et al.*, 1996; *Crooker et al.*, 1996], since on open field lines heat flux always flows away from the Sun. Accordingly, to test whether ϕ in Figure 2a gives true polarity in the sector with the magnetic cloud, we show the heat flux data from the Solar Wind Experiment (SWE) in of Figure 3a for February 7-12. This interval covers the cloud and the subsequent polarity change in ϕ. Figure 3b repeats the ϕ data, in this case with time running in the normal sense, from left to right. The heat flux pitch angle in Figure 3a is plotted relative to the magnetic field direction so that peak flux at 0° (180°) means heat flux parallel (antiparallel) to the field. In this format, a true polarity change from an away to a toward sector is represented by a shift of peak flux from 0° to 180°. Figure 3a shows a clear shift in this sense on February 8, at the beginning of the cloud, marking the true sector boundary. Since the heat flux peak continues at 180° throughout the plot, we conclude that the magnetic polarity change on February 10 is not a true polarity change. Thus the cloud was clearly associated with the sector boundary and brought it ~2 1/2 days earlier than predicted.

In retrospect, one can see that the original sector boundary choice on February 10, based on ϕ, was made because the field clearly rotated into the toward sector then but that the choice could have been earlier, since ϕ hovered at the ortho-Parker-spiral direction, between the two polarities, for more than a day prior to its toward rotation. This orientation, as noted below, suggests the presence of a transient structure.

In addition to showing the location of the true sector boundary, the heat flux data in Figure 3 also indicate that most of the cloud was magnetically open. In the labeled cloud interval, the heat flux electrons are primarily unidirectional. Bidirectional streaming indicating closed fields [e.g., *Gosling et al.*, 1987] occurred only for two brief intervals, one at the leading edge, where the flux maxima overlap, and one a few hours later. The extended bright regions beyond the cloud, primarily on February 11, signal distribution broadening in regions of high density or temperature, but there is little evidence of bidirectional streaming there.

Now that we have established that the cloud brought the sector boundary, the question arises as to what kind of structure spanned the region between the trailing edge of the cloud and the originally misidentified sector boundary. The ortho-Parker-spiral direction of ϕ in Figure 2 and the additional data we present in Figure 4 suggest that the region was part of a larger transient structure that includes the cloud as its leading edge, similar to the findings of *Crooker et al.* [1998] that led to the construction of Figure 1. The plot of magnetic latitude θ in the top panel of Figure 4 roughly shows the same kind of arched form, covering February 8-11, consistent with passing through both the leading edge and trailing leg of a flux rope loop [cf. *Marubashi*, 1997]. Following the arched form is a simultaneous rise in thermal speed and drop in density near 0830 UT on February 11, the signature of a stream interface. It marks the boundary between slow flow in the streamer belt and high-speed flow from the bordering coronal hole [e.g., *Gosling et al.*, 1978]. Thus the streamer belt appears to be filled with a transient structure in the form a flux rope loop spanning the interval between the leading edge of the cloud and the stream interface. By mapping this interval from the plot of ϕ down to the dashed Wind path on the source surface map in

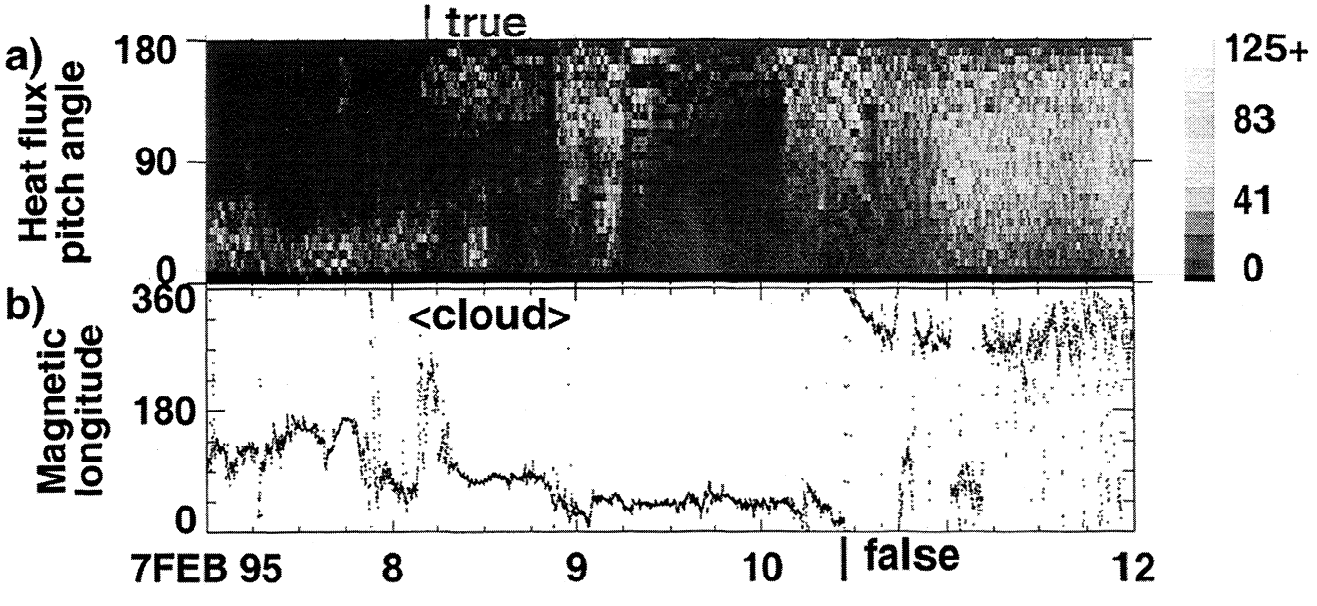

Figure 3. (a) Solar Wind Experiment (SWE) pitch angle spectrogram of electrons in the heat flux energy range (~200 eV) and (b) Magnetic Field Investigation (MFI) longitude angle ϕ covering five days. Short vertical lines mark true and false sector boundaries. The true sector boundary occurred where the heat flux direction changed from parallel (0°) to antiparallel (180°) to the magnetic field, at the leading edge of the magnetic cloud. The false sector boundary, determined from the polarity change in ϕ, trailed the cloud by ~2 days. Within the cloud, on February 8, two brief intervals of bidirectional streaming occurred, one at the leading edge, ~0300-0600, and one at ~0930-1230 UT.

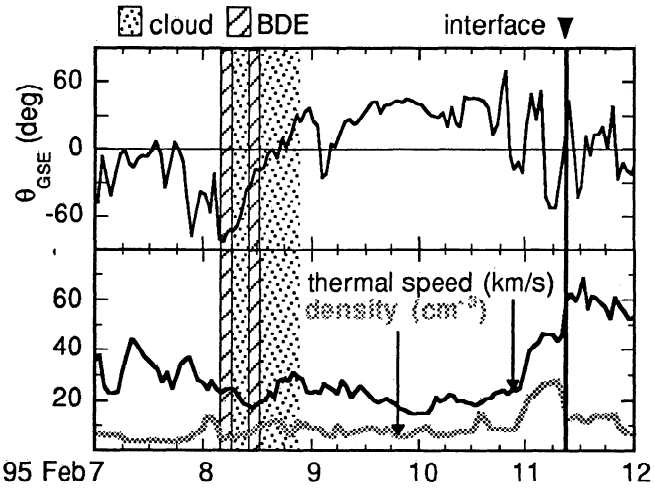

Figure 4. Time variations of magnetic latitude angle θ, thermal speed, and density. Hatched columns in shaded cloud interval indicate intervals of bidirectional electrons (BDEs). The rise in thermal speed and drop in density mark the stream interface at the boundary of the streamer belt.

Figure 2, we see that the structure, sketched as a white-filled area encompassing the neutral line, spans 45° of longitude. Like the sizes deduced by *Crooker et al.* [1998] for the cloud-associated intervals of bidirectional heat flux, this size is comparable to the average size of CMEs observed on the limb of the Sun [*Hundhausen*, 1993].

3. Cloud Topology

The results in section 2 show that the February 8, 1995, cloud and its trailing structure share the sector boundary association and magnetic signature identified by *Crooker et al.* [1998] in clouds observed by ISEE 3. At the same time, the results differ from the ISEE 3 results in two major ways. First, bidirectional heat flux did not even extend over the duration of cloud passage let alone over a period more than twice as long, covering the rise and fall of θ. Had the close association between the θ arch and the bidirectional electrons not been established earlier, arguing the significance of the ragged θ signature in this case would have been unconvincing. Second, the sector boundary came at the leading edge of the cloud rather than being carried by the cloud itself. These differences can be explained in terms of the same basic model proposed for the ISEE 3 clouds, illustrated in Figure 1, providing the closed topology is changed to a predominantly open topology.

Figure 5 illustrates the proposed magnetic topology for the February 8 cloud. Even though only a few selected field lines are shown, the geometry is intended to be the same as in Figure 1: A distorted flux rope loop lies at a sector boundary where the field polarity changes from away to toward, and the originally identified cloud is the leading leg of the loop. Again, dots mark spacecraft entry and exit points. In this case, however, the rope is not assumed to be entirely connected to the Sun at both ends. As indicated, one of the two helical field lines in the flux rope loop is open, presumably having merged with an adjacent open field line from the toward sector at the coronal end of the leading leg of the loop. This kind of mixed topology has been proposed by *Gosling et al.* [1995] as a consequence of the disordered reconnection seen in simulations of flux rope release, leading to eventual disconnection of a CME from the Sun. Reconnection of this type, specifically at the coronal end of the leg of the flux rope, has also been postulated by *Larson et al.* [1997] to explain Wind observations of mixed topologies in the October 1995 cloud. Additional similarities between the February and October clouds are discussed below.

Although schematic, the topology in Figure 5 is highly constrained by the observations. The outer helical field line is connected to the Sun at both ends, consistent with the interval of bidirectional electrons observed upon entry into the cloud. The inner helical field line is disconnected from the leading leg of the flux rope loop, which gives it toward polarity, even though locally the field points away from the Sun throughout the upper half of the helix. This configuration is consistent with three features of the observations. First, the lack of bidirectional electrons throughout most of the structure implies a predominance of open helical field lines. Second, the heat flux direction on these open field lines requires that their true polarity point toward the Sun. Third, the fact that the measured field direction points away from the Sun implies that the spacecraft passed above the midplane of the rope, at least in the leading leg of the loop, as would be expected for a tilted loop plane like that represented in Figure 1. Passage above the midplane has been confirmed by fitting the observations to a flux rope model [cf. *Lepping et al.*, 1996a]. We note that had passage been below the midplane of the cloud, the magnetic field measurement would have given the true polarity of the field.

The results discussed here, building on the results of *Crooker et al.* [1998], have important implications for the relationship between magnetic clouds and sector boundaries. As mentioned above, what seem like major differences between

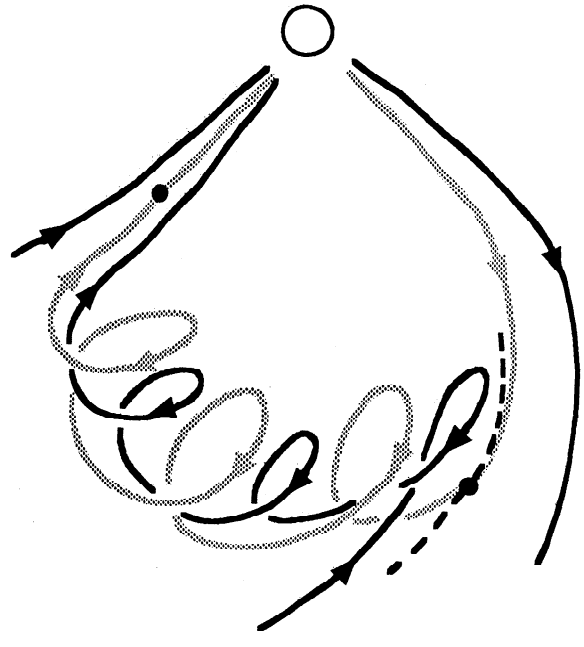

Figure 5. Schematic illustration of the magnetic field configuration in the February 1995 cloud. The black helix nested inside the gray one is open owing to reconnection in the leading leg of the flux rope loop. The dashed curve shows the resulting displacement of the sector boundary (cf. Figure 1). Black dots roughly indicate spacecraft entry and exit points.

the February 1995 cloud and those analyzed in the ISEE 3 data can be explained by the minor difference between Figures 1 and 5: only the latter contains open helical field lines. Had they been closed, no sector boundary signature would have appeared in the heat flux data at the beginning of the cloud. The heat flux would have been bidirectional throughout the rise in θ in the originally identified cloud and beyond, through its subsequent fall. Of greater significance, the observed magnetic polarity reversal, which agrees with the prediction from the source surface map (Figure 2), would have been treated as the sector boundary carried by the flux rope loop, as in Figure 1. We conclude that the displacement of the observed sector boundary from its predicted location to the location marked by the dashed curve in Figure 5 occurred as a result of reconnection that opened originally closed helical field lines. The common idea that the HCS is pushed aside by CMEs [e.g., *Gosling and McComas*, 1987; *Balogh et al.*, 1993] fits neither this case nor the basic model used to construct Figure 1. Observations to date support the idea presented here, that CME flux ropes are intrinsic parts of the HCS and, as a consequence, cannot push it aside [*Crooker et al.*, 1993; *Zhao and Hoeksema*, 1996; *Crooker and Intriligator*, 1996; *Crooker et al.*, 1998].

To close this section, we present support for the Figure 5 topology that is intimately related to its solar source and thus provides a bridge to the next section. Figure 6 shows observations from the 3-D Plasma and Energetic Particle experiment. Figure 6a is an energy spectrogram of the flux of energetic electrons streaming along the magnetic field, normalized by the background flux. It shows two impulsive energetic electron events near the leading edge of the cloud, identified by their characteristic dispersive signatures. Events of this type are associated with solar flares and type III radio emission and signal magnetic connection to an active region [*Lin*, 1985]. Similar events were found in the October 1995 cloud [*Larson et al.*, 1997]. The first of the two pronounced events (a much weaker event precedes it) began just prior to cloud entry and extended into the first bidirectional heat flux event, evident in Figure 6b, and the second impulsive event ended near the end of the same heat flux event. This pattern implies that the impulsive energetic electrons traveled from the Sun to the spacecraft along the fields at the leading leg of the flux rope loop, both ahead of the loop and inside it, but that they could reach the spacecraft only because those fields were connected to the Sun, as in the outer closed helix in Figure 5. The pattern also

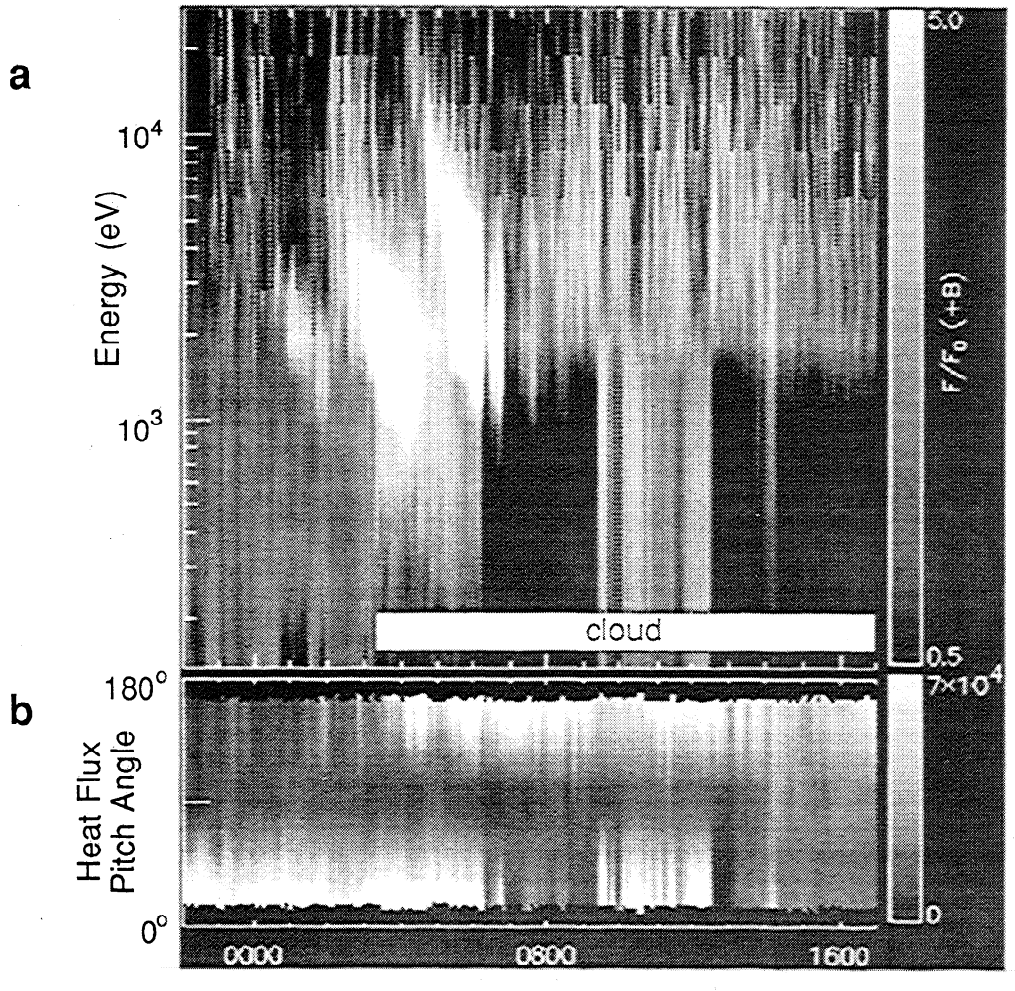

Figure 6. 3-D Plasma and Energetic Particle experiment spectrograms for February 8, 1995: (a) an energy spectrogram of the flux F of electrons streaming parallel to the magnetic field B, normalized by the background flux F_o, and (b) a pitch angle spectrogram. The two major bright patches in Figure 6a indicate impulsive electron events. These occurred near the beginning of the cloud, during the first of the two bidirectional heat flux events apparent in Figure 6b (cf. Figure 3).

implies that a portion of the leading leg was connected to an active region, as the next section confirms. Since an active region is a likely place for reconnection, this implication provides a reason for the disconnected helical fields in the leading leg required by the in situ plasma observations.

The mixed topology and deduced leg reconnection for the February 1995 cloud are similar to the findings of *Larson et al.* [1997] for the October 1995 cloud. These features contrast sharply with the extended closed topologies in clouds observed by ISEE 3 in 1978-1982. It remains to be tested whether this difference is a solar cycle variation, with closed topologies predominating near solar maximum.

4. Comparison with Solar Source Properties

The solar source for the February 1995 magnetic cloud structure seems clear in the Yohkoh soft X ray images on February 4, one of which is shown in Figure 7. A CME signature in the form of an eruptive arcade event [e.g., *McAllister and Hundhausen*, 1996; *Crooker and McAllister*, 1997] occurred along a neutral line (marked with a white curve) that switched direction as it passed through a bright active region near the center of the disk, a common configuration for CME sites [*McAllister et al.*, 1996; *Webb et al.*, 1997]. No other candidate solar event occurred during the previous 24 hours. The event began at about 1530 UT on February 4 as a low M-class, LDE (long-duration event) flare at the GOES spacecraft and was visible in the active region in the next available Yohkoh image at 1556 UT. Successive Yohkoh images show arcade loops, evident in Figure 7, expanding along the neutral line in both the northeast (up and left) and southeast (down and left) directions from the active region. These loops are believed to be newly regenerated portions of the helmet streamer belt following CME

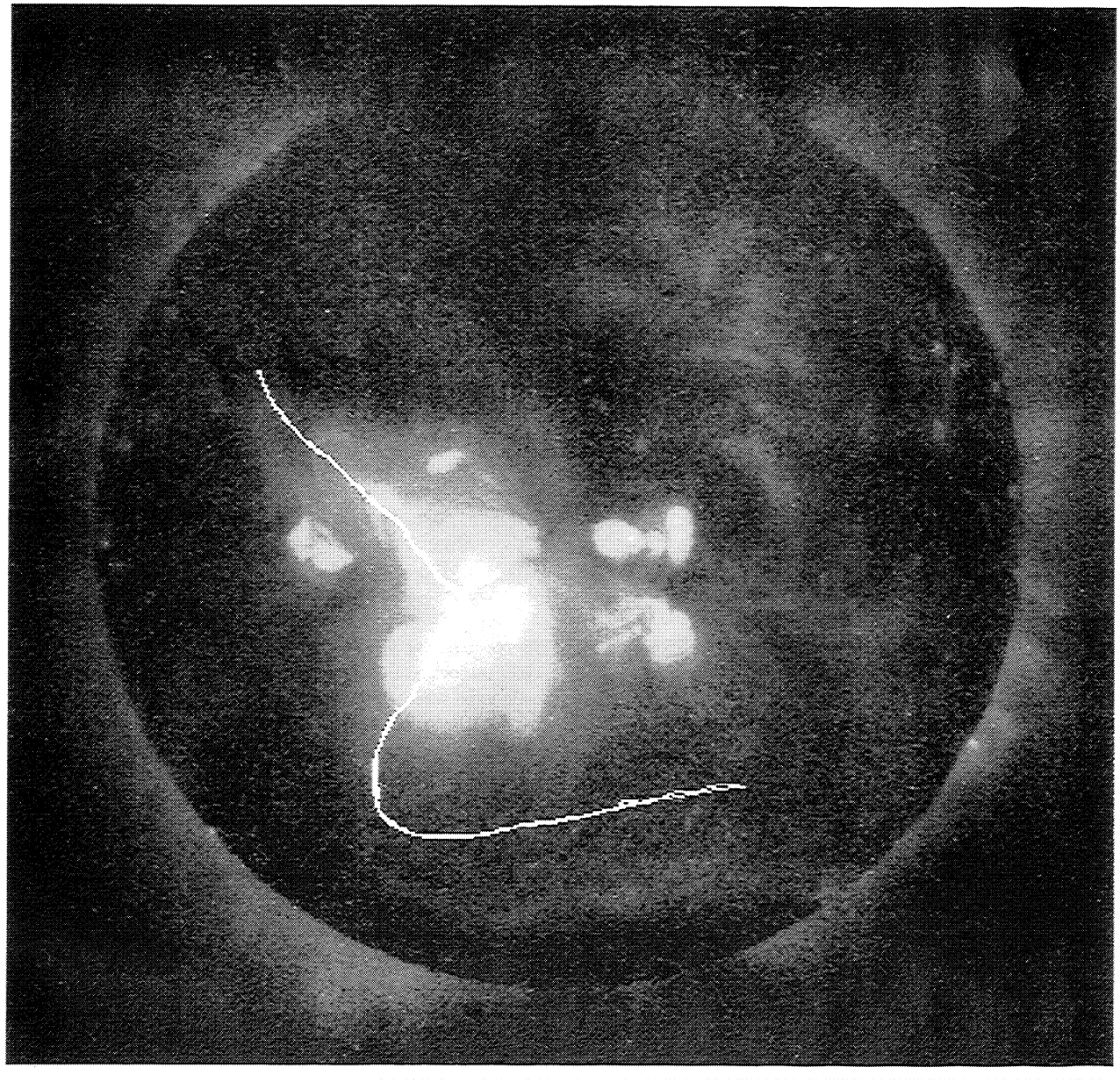

Figure 7. Yohkoh soft X ray image of the Sun on February 4, 1995, 1814 UT, showing the solar event associated with the February 8 magnetic cloud. The superposed white curve traces the photospheric neutral line, which kinks in an active region. The loops extending north and south of the kink form the arcade event that indicates CME liftoff. The dark regions on either side of the arcade event indicate coronal holes.

liftoff [e.g., *Hiei et al.*, 1993], consistent with the pattern of CME flux rope formation discussed in section 1.

The calculated transit time for the arcade event supports its choice as the source of the magnetic cloud. The start time of 1530 UT on February 4 and the arrival time at Wind of 0330 UT on February 8 implies an average transit speed of 500 km/s. Compared to the in situ speed at the leading edge of the cloud of 450 km/s, the implied average speed is reasonable and consistent with minor deceleration between the Sun and 1 AU [cf. *Cliver et al.*, 1990].

Additional evidence for the February 4 arcade event as the source of the February 8 magnetic cloud can be found in Mauna Loa white light synoptic maps of the corona, which show brightness contours that outline the streamer belt (courtesy of J. Burkepile, High Altitude Observatory). The maps from the east and west limbs of the Sun for Carrington Rotation 1892 (not shown) are strikingly different. The streamer belt in the identified source region was much brighter on the west limb, consistent with formation of a new helmet streamer following CME liftoff between limb passages.

The active region in the Yohkoh image in Figure 7 continued to be active for many days. Specifically, relevant to the impulsive electron events described in section 3, the Yohkoh images from 0238 to 0256 UT on February 8 show expansions of the loops just south of the arcade. This time interval coincides with the beginning of the first impulsive event in Figure 6. A gap in the Yohkoh data following this interval prevents further comparison.

Below we relate geometrical and topological properties of the February 4 source event to those of the magnetic cloud obtained from modeling. First, however, we note that most of the arcade event occurred below the ecliptic plane, which runs through the middle of the solar disk in Figure 7. Consequently, the relevant part of the arcade event is that portion closest to the ecliptic plane, specifically, the loops branching northeast from the active region. A flux rope arising from this portion would have its leading leg rooted in an area that includes the active region, consistent with the impulsive electron observations and the topology in Figure 5.

The first property we address is magnetic helicity [cf. *Marubashi*, 1986; *Rust*, 1994; *Bothmer and Rust*, 1997]. Following *Martin and McAllister* [1997, 1998], we observe that the northeastern loops have a left-handed skew, as expected for a northern hemisphere source, even though they are located in the southern hemisphere. Nevertheless, this finding agrees with the left-handed helicity observed in the cloud, as predicted by *Martin and McAllister* [1997, 1998].

A second prediction borne out in the cloud is the southward magnetic field at the leading edge, which is the same direction as the solar dipolar field at this phase of the solar cycle. A correlation between the leading field direction in clouds and the solar dipolar field was first suggested by *Marubashi* [1986] and established by *Bothmer and Rust* [1997] and *Bothmer and Schwenn* [1998] and has been confirmed by *Mulligan et al.* [1998]. Although there are exceptions to the correlation, the pattern emerges as a natural consequence of CME formation in the basic heliospheric topology discussed in section 1.

A third cloud property that can be matched to source characteristics is the inclination of the cloud axis with respect to the ecliptic plane. From the model fit to a force free flux rope, we obtain an inclination of 10°. (The original value of -10° obtained by *Lepping et al.* [1996a] was calculated without benefit of subsequently available baseline corrections for the north-south field component.) This axis should be aligned with the axis of the source event, according to the basic heliospheric topology discussion in section 1. The source event axis is the northern branch of the neutral line in Figure 7, which is inclined by 45° to the ecliptic plane. Thus the cloud axis differs from the predicted axis by 35°. This difference lies well within the observed range of differences between cloud axes and associated neutral-line-aligned filaments found in earlier studies [*Marubashi*, 1986, 1997; *Zhao and Hoeksema*, 1998].

To clarify the axis geometry, we place it in the context of the background magnetic configuration by using results from an MHD model calculated for this period [*Linker and Mikic*, 1997]. The model uses photospheric magnetic field data from synoptic charts generated from measurements at the National Solar Observatory at Kitt Peak to specify the boundary condition on the radial magnetic field. Consequently, unlike the Yohkoh images, the model results are time-aliased; but they give an excellent view of the overall pattern in which specific events occurred. Figure 8 shows a view based on a synoptic chart with February 4 near central meridian, constructed to approximately match the Yohkoh image in Figure 7. Calculated magnetic field lines extend from the solar surface, where dark shading indicates the location of coronal holes, comparable to the dark regions in Figure 7. The horizontal curved line near the equator marks the projection of the calculated HCS, comparable to the neutral line on the source surface map in Figure 2 except for somewhat smaller latitudinal excursions [*Linker and Mikic*, 1997].

Figure 8 displays the basic heliospheric topology and, at the same time, illustrates the complexities of the magnetic configuration closer to the Sun than the source surface, at a level where CMEs form. Comparing Figure 8 to Figure 7, we see that the CME source was located in a coronal arcade encircling the Sun as the streamer belt. The streamer belt section near the source was sandwiched between an isolated, low-latitude coronal hole to the northwest, with northern hemisphere away polarity, and a coronal hole extension from the southern polar hole to the southeast, with toward polarity. This configuration, although complicated, reflects the dipolar structure of the heliosphere and is consistent with the sector structure associated with the cloud.

Returning to the issue of nonalignment of the cloud and source axes, we see that in the vicinity of the source event the HCS projection in Figure 8 has a lower inclination than the arcade axis, which follows the photospheric neutral line in Figure 7. These features are brought together with a superposed cloud axis for comparison in Figure 9. The cloud axis is centered over the source region, slightly below the ecliptic plane, consistent with spacecraft intersection above the axis. Figure 9 shows the 35° angle between the cloud axis and the neutral line but only a 24° angle between the cloud axis and the projected HCS. Thus, if the cloud axis was originally aligned with the neutral line, subsequent realignment with the HCS as the cloud moved outward would have decreased the inclination by 11°. The angles discussed here are, of course, subject to model uncertainties, but, at the very least, they are consistent with the predictions.

5. Conclusions

The primary conclusion we draw from this study is that sector boundaries can be substantially transformed during passage of a magnetic cloud owing to the presence of helical field lines

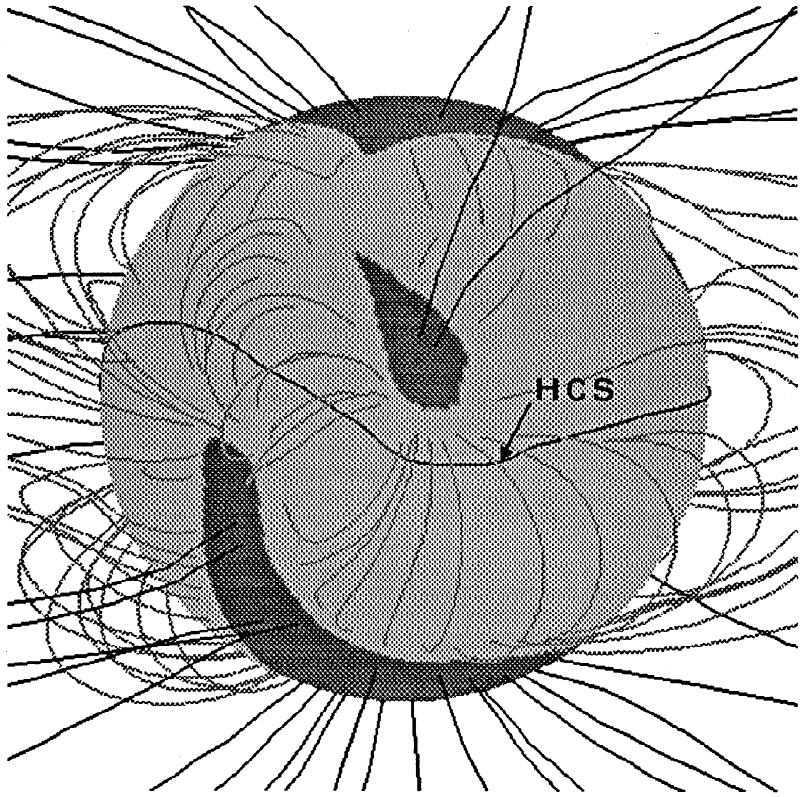

Figure 8. Solar magnetic field lines from an MHD model for the same time period and viewing point shown in the Yohkoh image in Figure 7. Open field lines are black, and closed field lines are gray. Dark shading on the solar surface indicates the calculated coronal hole areas, which provide a good match to the dark regions in Figure 7. The curve threading the central arcade marks the projection of the model heliospheric current sheet (HCS).

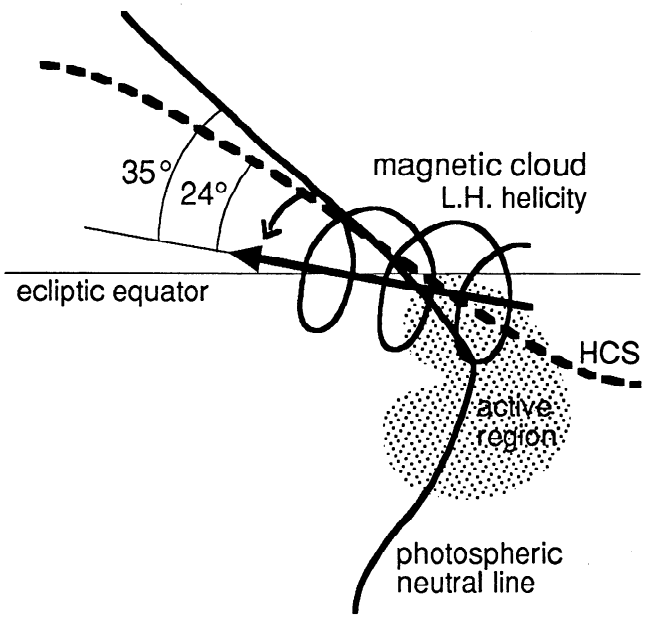

Figure 9. Schematic diagram combining the photospheric neutral line (solid) and the area of the active region arcade event from Figure 7 and the HCS (dashed) from Figure 8 with the projected magnetic cloud position and axis orientation. The left-hand helicity of the cloud agrees with the skew observed in the northward extending arcade event, and the cloud axis lies within 35° of alignment with the neutral line and 24° of alignment with the HCS.

within the cloud that are connected only to the following sector. This sector boundary displacement is thus accomplished by a topological reconfiguration rather than a pushing aside of the HCS by the cloud. Whether or not the sector boundary displacement is apparent in the magnetic field data depends on where the spacecraft passes through the structure. In the case presented here, the true sector boundary only became apparent when the direction of the electron heat flux relative to the direction of the magnetic field was taken into account. Had the spacecraft passed below rather than above the cloud axis, the magnetic field data would have reflected the true sector boundary location. Furthermore, had the helical fields in the cloud been closed and host to counterstreaming electrons, the dominant heat flux direction, indicating the direction of closest solar connection [cf. *Kahler et al.*, 1996], presumably would have implied agreement between the magnetic and true polarity changes, consistent with Figure 1. In this view, magnetic clouds preserve the sector structure except when they become magnetically open.

Another important conclusion is that the present results, taken together with the results of *Zhao and Hoeksema* [1996] and *Crooker et al.* [1998], support a straightforward view of the relationship between magnetic clouds, sector boundaries, and the solar-dipole-dominated topology of the heliosphere.

Acknowledgments. We thank K. W. Ogilvie for help in implementing this project. The research was supported by NASA GSFC under PR S-78748-Z, PR S-96491-Z, and grant NAG5-7049 and by the National Science Foundation under grant ATM94-21814 and under the auspices

of the National Center for Atmospheric Research. The Wind 3DP data analysis at Berkeley is supported by NASA grant NAG5-2815.

The Editor thanks Z. Smith and K. Marubashi for their assistance in evaluating this paper.

References

Balogh, A., G. Erdos, R. J. Forsyth, and E. J. Smith, The evolution of the interplanetary sector structure in 1992, *Geophys. Res. Lett., 20*, 2331-2334, 1993.

Bothmer, V., and D. M. Rust, The field configuration of magnetic clouds and the solar cycle, in *Coronal Mass Ejections, Geophys. Monogr. Ser.*, vol. 99, edited by N. U. Crooker, J. A. Joselyn, and J. Feynman, pp. 137-146, AGU, Washington, D. C., 1997.

Bothmer, V., and R. Schwenn, The structure and origin of magnetic clouds in the solar wind, *Ann. Geophys., 16*, 1-24, 1998.

Burton, M. E., N. U. Crooker, G. L. Siscoe, and E. J. Smith, A test of source-surface model predictions of heliospheric current sheet inclination, *J. Geophys. Res., 99*, 1-9, 1994.

Cliver, E. W., J. Feynman, and H. B. Garrett, An estimate of the maximum speed of the solar wind, 1938-1989, *J. Geophys. Res., 95*, 17,103-17,112, 1990.

Crooker, N. U., and D. S. Intriligator, A magnetic cloud as a distended flux-rope occlusion in the heliospheric current sheet, *J. Geophys. Res., 101*, 24,343-24,348, 1996.

Crooker, N. U., and A. H. McAllister, Transients associated with recurrent storms, *J. Geophys. Res., 102*, 14,041-14,047, 1997.

Crooker, N. U., G. L. Siscoe, S. Shodhan, D. F. Webb, J. T. Gosling, and E. J. Smith, Multiple heliospheric current sheets and coronal streamer belt dynamics, *J. Geophys. Res., 98*, 9371-9381, 1993.

Crooker, N. U., M. E. Burton, G. L. Siscoe, S. W. Kahler, J. T. Gosling, and E. J. Smith, Solar wind streamer belt structure, *J. Geophys. Res., 101*, 24,331-24,341, 1996.

Crooker, N. U., J. T. Gosling, and S. W. Kahler, Magnetic clouds at sector boundaries, *J. Geophys. Res., 103*, 301-306, 1998.

Gosling, J. T., and D. J. McComas, Field line draping about fast coronal mass ejecta: A source of strong out-of-the-ecliptic interplanetary magnetic fields, *Geophys. Res. Lett., 14*, 355-358, 1987.

Gosling, J. T., J. R. Asbridge, S. J. Bame, and W. C. Feldman, Solar wind stream interfaces, *J. Geophys. Res., 83*, 1401-1412, 1978.

Gosling, J. T., D. N. Baker, S. J. Bame, W. C. Feldman, and R. D. Zwickl, Bidirectional solar wind electron heat flux events, *J. Geophys. Res., 92*, 8519-8535, 1987.

Gosling, J. T, J. Birn, and M. Hesse, Three-dimensional magnetic reconnection and the magnetic topology of coronal mass ejection events, *Geophys. Res. Lett., 22*, 869-872, 1995.

Hiei, E., A. J. Hundhausen, and D. G. Sime, Reformation of a coronal helmet streamer by magnetic reconnection after a coronal mass ejection, *Geophys. Res. Lett., 20*, 2785-2788, 1993.

Howard, R. A., et al., Observations of CMEs from SOHO/LASCO, in *Coronal Mass Ejections, Geophys. Monogr. Ser.*, vol. 99, edited by N. U. Crooker, J. A. Joselyn, and J. Feynman, pp. 17-26, AGU, Washington, D. C., 1997.

Hundhausen, A. J., The sizes and locations of coronal mass ejections: SMM observations from 1980 and 1984-1989, *J. Geophys. Res., 98*, 13,177-13,200, 1993.

Kahler, S., and R. P. Lin, The determination of interplanetary magnetic field polarities around sector boundaries using E>2 keV electrons, *Geophys. Res. Lett., 21*, 1575-1578, 1994.

Kahler, S., and R. P. Lin, An examination of directional discontinuities and magnetic polarity changes around interplanetary sector boundaries using E>2 keV electrons, *Sol. Phys., 161*, 183-195, 1995.

Kahler, S. W., N. U. Crooker, and J. T. Gosling, The topology of intrasector reversals of the interplanetary magnetic field, *J. Geophys. Res., 101*, 24,373-24,382, 1996.

Larson, D. E., et al., Tracing the topology of the October 18-20, 1995 magnetic cloud with ~0.1 - 10^2 keV electrons, *Geophys. Res. Lett., 24*, 1911-1914, 1997.

Lepping, R. L., A. Szabo, K. W. Ogilvie, R. J. Fitzenreiter, L. F. Burlaga, and A. J. Lazarus, WIND and IMP-8 observations of a magnetic cloud - magnetosphere interaction, *Geophys. Res. Lett., 23*, 1195-1198, 1996a.

Lepping, R. L., A. Szabo, M. Peredo, and J. T. Hoeksema, Large-scale properties and solar connection of the heliospheric current and plasma sheets: WIND observations, *Geophys. Res. Lett., 23*, 1199-1202, 1996b.

Lin, R. P., Energetic solar electrons in the interplanetary medium, *Solar Phys., 100*, 537-561, 1985.

Linker, J. A., and Z. Mikic, Extending coronal models to Earth orbit, in *Coronal Mass Ejections, Geophys. Monogr. Ser.*, vol. 99, edited by N. U. Crooker, J. A. Joselyn, and J. Feynman, pp. 269-277, AGU, Washington, D. C., 1997.

Martin, S. F., and A. H. McAllister, Predicting the sign of helicity in erupting filaments and coronal mass ejections, in *Coronal Mass Ejections, Geophys. Monogr. Ser.*, vol. 99, edited by N. U. Crooker, J. A. Joselyn, and J. Feynman, pp. 127-138, AGU, Washington, D. C., 1997.

Martin, S. F., and A. H. McAllister, The chirality of X ray coronal arcades overlying quiescent filaments, *Astrophys. J.*, in press, 1998.

Marubashi, K., Structure of the interplanetary magnetic clouds and their solar origins, *Adv. Space Res., 6*(6), 335-338, 1986.

Marubashi, K., Interplanetary magnetic flux ropes and solar filaments, in *Coronal Mass Ejections, Geophys. Monogr. Ser.*, vol. 99, edited by N. U. Crooker, J. A. Joselyn, and J. Feynman, pp. 147-156, AGU, Washington, D. C., 1997.

McAllister, A. H., and A. J. Hundhausen, The relation of Yohkoh coronal arcade events to coronal streamers and CMEs, in *Solar Drivers of Interplanetary and Terrestrial Disturbances*, edited by K. S. Balasubramaniam, S. L. Keil, and R. N. Smartt, pp. 171-179, Astron. Soc. of the Pacific, San Francisco, Calif., 1996.

McAllister, A. H., A. J. Hundhausen, J. T. Burkepile, P. McIntosh, and E. Hiei, Declining phase coronal evolution: The statistics of X ray arcades, in *Magnetodynamic Phenomena in the Solar Atmosphere - Prototypes of Stellar Magnetic Activity*, edited by Y. Uchida, T. Kosugi, and H. Hudson, pp. 123-124, Kluwer Acad., Norwell, Mass., 1996.

Mulligan, T., C. T. Russell, and J. G. Luhmann, Solar cycle evolution of the structure of magnetic clouds in the inner heliosphere, *Geophys. Res. Lett., 25*, 2959-2963, 1998.

Pneuman, G. W., and R. A. Kopp, Gas-magnetic field interactions in the solar corona, *Sol. Phys., 18*, 258, 1971.

Rust, D. M., Spawning and shedding helical magnetic fields in the solar atmosphere, *Geophys. Res. Lett., 21*, 241-244, 1994.

Webb, D. F., S. W. Kahler, P. S. McIntosh, and J. A. Klimchuk, Large-scale structures and multiple neutral lines associated with coronal mass ejections, *J. Geophys. Res., 102*, 24,161-24,174, 1997.

Zhao, X.-P., and J. T. Hoeksema, Effect of coronal mass ejections on the structure of the heliospheric current sheet, *J. Geophys. Res., 101*, 4825-4834, 1996.

Zhao, X.-P., and J. T. Hoeksema, Central axial field direction in magnetic clouds and its relation to southward interplanetary magnetic field events and dependence on disappearing solar filaments, *J. Geophys. Res., 103*, 2077-2083, 1998.

N. U. Crooker, Center for Space Physics, Boston University, 725 Commonwealth Avenue, Boston, MA 02215. (e-mail: crooker@buasta.bu.edu)

R. J. Fitzenreiter, R. P. Lepping and A. Szabo, Laboratory for Extraterrestrial Physics, NASA Goddard Space Flight Center, Greenbelt, MD 20771. (e-mail: u3rjf@leprjf.gsfc.nasa.gov; rpl@leprpl1.gsfc.nasa.gov; asz@leprpl1.gsfc.nasa.gov)

D. E. Larson and R. P. Lin, Space Sciences Laboratory, University of California, Berkeley, CA 94720. (e-mail: davin@ssl.berkeley.edu; rlin@ssl.berkeley.edu)

A. J. Lazarus and J. T. Steinberg, Center for Space Research, Rm 37-687, Massachusetts Institute of Technology, Cambridge, MA 02139. (e-mail: ajl@space.mit.edu; jts@space.mit.edu)

J. A. Linker and Z. Mikic, Science Applications International Corporation, 10260 Campus Point Drive, San Diego, CA 92121. (e-mail: linker@iris023.saic.com; mikic@iris023.saic.com)

A. H. McAllister, HAO/NCAR, Box 3000, Boulder, CO 80304. (e-mail: ahm@hao.ucar.edu)

(Received March 3, 1998: revised June 26, 1998:
accepted July 6, 1998.)